

On the convergence properties of GAN training

Lars Mescheder*

*Autonomous Vision Group
MPI Tübingen*

Abstract

Recent work has shown local convergence of GAN training for absolutely continuous data and generator distributions. In this note we show that the requirement of absolute continuity is necessary: we describe a simple yet prototypical counterexample showing that in the more realistic case of distributions that are not absolutely continuous, unregularized GAN training is generally not convergent. Furthermore, we discuss recent regularization strategies that were proposed to stabilize GAN training. Our analysis shows that while GAN training with instance noise or gradient penalties converges, Wasserstein-GANs and Wasserstein-GANs-GP with a finite number of discriminator updates per generator update do in general not converge to the equilibrium point. We explain these results and show that both instance noise and gradient penalties constitute solutions to the problem of purely imaginary eigenvalues of the Jacobian of the gradient vector field. Based on our analysis, we also propose a simplified gradient penalty with the same effects on local convergence as more complicated penalties.

1 Introduction

Generative Adversarial Networks (GANs) [3] are powerful latent variable models that can be used to learn complex real-world distributions. Especially for natural images, GANs have emerged as one of the dominant approaches for generating new realistically looking samples after the model has been trained on some fixed dataset.

However, while very powerful, GANs can be hard to train and in practice it is often observed that gradient descent based GAN optimization does not lead to convergence. As a result, a lot of recent research has focused on finding better training algorithms [2, 4, 8, 16, 14] for GANs as well as gaining better theoretical understanding of their training dynamics [2, 1, 10, 11, 6].

Despite practical advances, the training dynamics of GANs are still not completely understood. Recently, it was shown [10, 11] that local convergence and stability properties of GAN training can be analyzed by examining the

*Electronic address: lars.mescheder@tue.mpg.de

eigenvalues of the Jacobian of the the associated gradient vector field of the GAN training objective: if the Jacobian has only eigenvalues with negative real-part at the equilibrium point, GAN training converges locally for small enough learning rates. On the other hand, if the Jacobian has eigenvalues on the imaginary axis, it is generally not locally convergent. Moreover, in [10] it is shown that if there are eigenvalues close but not on the imaginary axis, the training algorithm might require extremely small learning rates to achieve convergence. While the authors of [10] empirically validate the presence of eigenvalues close to the imaginary axis on an example problem, this does not answer the question if this is a general phenomenon and if yes, whether it is indeed the root cause for the training instabilities that people observe in practice.

A partial answer to this question is given in [11], where it is shown that for absolutely continuous data and generator distributions¹ and provided that some other suitable assumptions hold, all eigenvalues of the Jacobian have negative real-part. As a result, GANs are locally convergent for small enough learning rates in this case. Unfortunately, however, the assumption of absolute continuity is not true for the most common use cases of GANs, where both distributions typically lie on low dimensional manifolds [1].

In this note we show that this assumption is indeed necessary: by considering a simple yet prototypical example of GAN training we analytically show that GAN training is generally neither locally nor globally convergent. We also discuss how recent techniques for stabilizing GAN training affect local convergence on our example problem. Our findings show that neither Wasserstein GANs (WGANs) [2] nor Wasserstein GANs with Gradient Penalty (WGAN-GP) [4] nor DRAGAN [8] converge on this simple example for a fixed number of discriminator updates per generator update. On the other hand, we found that instance noise [16, 1], gradient penalties [14] and consensus optimization [10] lead to local convergence.

Based on our analysis, we also introduce a simplified gradient penalty that we found to work well in practice, confirming our hypothesis that eigenvalues with zero real part are indeed one of the root causes for the instabilities commonly observed when training generative adversarial networks.

In summary, our contributions are as follows:

- We identify a simple yet prototypical counterexample showing that gradient descent based GAN optimization is generally not convergent
- We identify the main obstacles for local convergence and discuss if and how recently introduced regularization techniques stabilize training
- We describe a simplified gradient penalty that leads to local convergence

All derivations and proofs can be found in the appendix.

¹ The authors of [11] also prove local convergence for a slightly more general family of probability distributions where the support of the generator is equal to the support of the true data distribution near the equilibrium point. Alternatively, it is shown that their results also hold when the discriminator satisfies certain smoothness conditions. However, the conditions are usually hard to satisfy in practice without prior knowledge about the support of the true data distribution.

2 Instabilities in GAN training

Simple experiments, simple theorems are the building blocks that help us understand more complicated systems.

Ali Rahimi - Test of Time Award speech, NIPS 2017

2.1 Background

GANs are defined by a min-max two-player game between a discriminative network $D_\psi(x)$ and generative network $G_\theta(z)$. While the discriminator tries to distinguish between real data point and data points produced by the generator, the generator tries to fool the discriminator. It can be shown [3] that if both the generator and discriminator are powerful enough to approximate any real-valued function, the unique Nash-equilibrium of this two player game is given by a generator that produces the true data distribution and the zero discriminator.

In the notation of [11], the training objective for the two players can be described by an objective function of the form

$$L(\theta, \psi) = \mathbb{E}_{p(z)} [f(D_\psi(G_\theta(z)))] + \mathbb{E}_{p_{\mathcal{D}}(x)} [f(-D_\psi(x))] \quad (1)$$

for some real-valued function f . The common choice $f(t) = -\log(1 + \exp(-t))$ leads to the loss function considered in the original GAN paper [3]. For technical reasons we assume that f is continuously differentiable and satisfies $f'(t) \neq 0$ for all $t \in \mathbb{R}$.

The goal of the generator is to minimize this loss whereas the discriminator tries to maximize it. Our goal when training GANs is to find a Nash-equilibrium, i.e. a parameter assignment (θ^*, ψ^*) where neither the discriminator nor the generator can improve their utilities unilaterally.

GANs are usually trained using simultaneous or alternating gradient descent. Both algorithms can be described as fixed point algorithms [10] that apply some operator $F_h(\theta, \psi)$ to the parameter values (θ, ψ) of the generator and discriminator respectively. For example, simultaneous gradient descent corresponds to the operator

$$F_h(\theta, \psi) = \begin{pmatrix} \theta - h\nabla_\theta L(\theta, \psi) \\ \psi + h\nabla_\psi L(\theta, \psi) \end{pmatrix}. \quad (2)$$

Similarly, alternating gradient descent can be described by an operator $F_h = F_{2,h} \circ F_{1,h}$ with

$$F_{1,h}(\theta, \psi) = \begin{pmatrix} \theta - h\nabla_\theta L(\theta, \psi) \\ \psi \end{pmatrix} \text{ and } F_{2,h}(\theta, \psi) = \begin{pmatrix} \theta \\ \psi + h\nabla_\psi L(\theta, \psi) \end{pmatrix} \quad (3)$$

Recently, it was shown [10, 11] that local convergence of GAN training near an equilibrium point (θ^*, ψ^*) can be understood by looking at the spectrum of the Jacobian $F'(\theta^*, \psi^*)$ at the equilibrium: if $F'(\theta^*, \psi^*)$ has eigenvalues with absolute value bigger than 1, the training algorithm will generally not converge to (θ^*, ψ^*) . On the other hand, if all eigenvalues have absolute value smaller

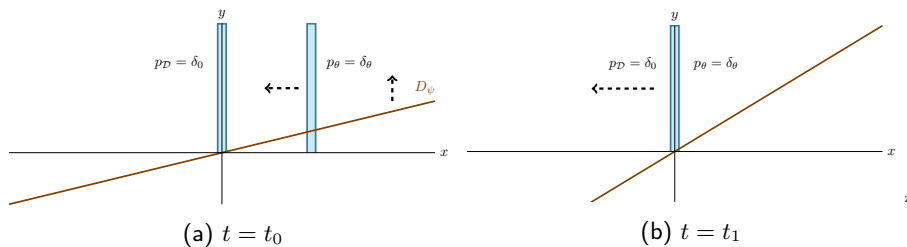


Fig. 1: Visualization of the counterexample showing that in the general case, gradient descent GAN optimization is not convergent: (a) In the beginning, the discriminator pushes the generator towards the true data distribution and the discriminator’s slope increases. (b) When the generator reaches the target distribution, the slope of the discriminator is strongest, pushing the generator away from the target distribution. All in all, this results in oscillatory training dynamics that never converge.

than 1, the training algorithm will be convergent to (θ^*, ψ^*) with linear rate $\mathcal{O}(|\lambda_{\max}|^n)$ where λ_{\max} is the eigenvalue of $F'(\theta^*, \psi^*)$ with the biggest absolute value [10].

For example, for simultaneous gradient descent linear convergence can be achieved if and only if all all eigenvalues of the Jacobian of the gradient vector field

$$v(\theta, \psi) = \begin{pmatrix} -\nabla_{\theta} L(\theta, \psi) \\ \nabla_{\psi} L(\theta, \psi) \end{pmatrix} \quad (4)$$

have negative real part [10]. This was also considered in [11] where the authors examine the asymptotic case of step sizes h that go to 0 and prove convergence for distributions that locally have the same support under certain regularity assumptions.

If all eigenvalues $F'(\theta^*, \psi^*)$ are on the unit circle, the algorithm can be convergent, divergent or neither, but if it is convergent it will generally converge with a sublinear rate.

2.2 A minimal counter example

In this section, we describe a simple yet prototypical counterexample which shows that in the general case, unregularized GAN training is neither locally nor globally convergent.

In our counterexample, the true data distribution $p_{\mathcal{D}}$ is given by $p_{\mathcal{D}} = \delta_0$ and the generator is given by $p_{\theta} = \delta_{\theta}$. We consider a simple linear discriminator given by $D_{\psi}(x) = \psi \cdot x$. This situation is visualized in Figure 1. In this setup, the GAN training objective (1) is given by

$$L(\theta, \psi) = f(\theta\psi) + f(0) \quad (5)$$

We show that the training dynamics of GANs lead to divergent behavior in this simple setup.

Lemma 1. *The unique equilibrium point of the training objective in (5) is given by $\phi = \psi = 0$. Moreover, the Jacobian of the gradient vector field at the equilibrium point has the two eigenvalues $\pm f'(0)i$ which are both on the imaginary axis.*

We now take a closer look at the training dynamics produced by various algorithm for training this GAN. First, we consider the (idealized) continuous system

$$\begin{pmatrix} \dot{\theta}(t) \\ \dot{\psi}(t) \end{pmatrix} = \begin{pmatrix} -\nabla_{\psi} L(\theta, \psi) \\ \nabla_{\theta} L(\theta, \psi) \end{pmatrix} \quad (6)$$

which corresponds to training the GAN with infinitely small learning rate.

While Lemma 1 shows that the continuous system in (6) is generally not linearly convergent towards the equilibrium point, it could in principle converge with a sublinear convergence rate. However, this is not the case as the next lemma shows:

Lemma 2. *The integral curves of the gradient vector field $v(\theta, \psi)$ do not converge to the Nash-equilibrium. More specifically, every integral curve $(\theta(t), \psi(t))$ of the gradient vector field $v(\theta, \psi)$ satisfies*

$$\theta(t)^2 + \psi(t)^2 = \text{const} \quad (7)$$

for all $t \in [0, \infty)$.

Note that our results do not contradict the results of [11] and [6]: our example violates Assumption IV in [11] that the support of the generator distribution is equal to the support of the true data distribution near the equilibrium. It also violates the assumption in [6] that the optimal discriminator parameter vector is a continuous function of the current generator parameters². In fact, for most generator parameters there is not even an optimal discriminator parameter vector in our example. Indeed, we found that two-time scale updates as suggested in [6] did not help convergence towards the Nash-equilibrium (see Figure 10 in the appendix). However, our example seems to be a prototypical situation for (unregularized) GAN training which usually deals with distributions that are concentrated on lower dimensional manifolds [1].

We now take a closer look at the discretized system.

Lemma 3. *For simultaneous gradient descent, the Jacobian of the update operator $F_h(\theta, \psi)$ has eigenvalues $\lambda_{1/2} = 1 \pm hf'(0)i$ with absolute values $\sqrt{1 + h^2 f'(0)^2}$ at the Nash equilibrium. Independently of the learning rate, simultaneous gradient descent is therefore not stable near the Nash-equilibrium. Even stronger, for every initial condition and learning rate $h > 0$, the norm of the iterates (θ_k, ψ_k) obtained by simultaneous gradient descent is monotonically increasing.*

² This assumption is usually even violated by Wasserstein-GANs, as the optimal discriminator parameter vector as a function of the current generator parameters can have discontinuities near the Nash-equilibrium. See Section 3.2 for details.

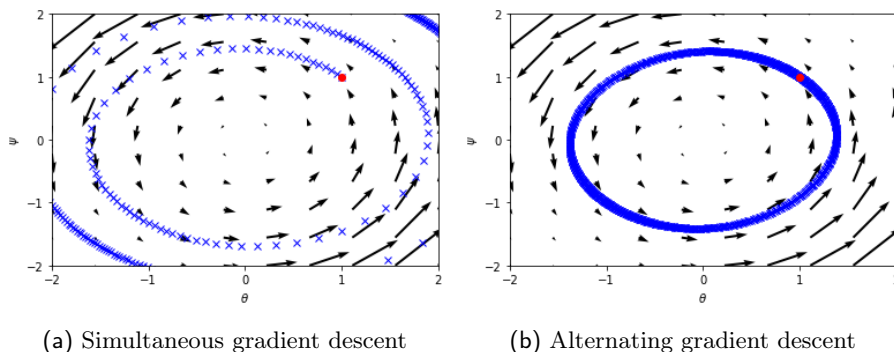


Fig. 2: Training behavior of GAN on the example problem.

The behavior of simultaneous gradient descent on our example problem is visualized in Figure 2a.

Similarly, for alternating gradient descent we have

Lemma 4. *For alternating gradient descent with n_g generator and n_d discriminator updates, the Jacobian of the update operator $F_h(\theta, \psi)$ has eigenvalues*

$$\lambda_{1/2} = 1 - \frac{n_g n_d h^2}{2} f'(0)^2 \pm \sqrt{\left(1 - \frac{n_g n_d h^2}{2} f'(0)^2\right)^2 - 1}. \quad (8)$$

For $\sqrt{n_g n_d} h f'(0) \leq 2$, all eigenvalues are hence on the unit circle. Moreover for $\sqrt{n_g n_d} h f'(0) > 2$, there are eigenvalues outside the unit ball.

Even though Lemma 4 shows that alternating gradient descent does not converge linearly to the Nash-equilibrium, it could in principle converge with a sublinear convergence rate. However, this is very unlikely because - as Lemma 2 shows - even the continuous system does not converge. Indeed, we empirically found that alternating gradient descent oscillates in stable cycles around the equilibrium and shows no sign of convergence (Figure 2b).

2.3 Where do instabilities come from?

Our simple example shows that naive gradient based GAN optimization is generally not convergent towards the equilibrium point. To get a better understanding of what can go wrong for more complicated GANs, it is instructive to analyze these instabilities in depth for this simple example problem.

To understand the instabilities, we have to take a closer look at the oscillatory behavior that GANs exhibit both on our example problem and for more complex systems. An intuitive explanation for the oscillations is given in Figure 1: when the generator is far from the true data distribution, the discriminator pushes the generator towards the true data distribution. At the same time, the discriminator becomes better at distinguishing real from generated

samples, which increases the discriminator’s slope (Figure 1a). Now, when the generator reaches the target distribution (Figure 1b), the slope of the discriminator is strongest, pushing the generator away from the target distribution. As a result, the generator moves away again from the true data distribution and the discriminator has to change its slope from positive to negative. After a while, we end up with a similar situation as in the beginning of training, only on the other side of the true data distribution. This process now repeats indefinitely and the training dynamics never converge to the equilibrium point.

Another way to look at this is to consider the local behavior of the training algorithm near the Nash-equilibrium. Indeed, near the Nash-equilibrium, there is nothing that pushes the discriminator towards having zero slope on the true data distribution. Even if the generator is initialized *exactly* on the target distribution, there is no incentive for the discriminator to move to the equilibrium discriminator. In addition, if the discriminator is close to the equilibrium discriminator, there is nothing that pushes the generator towards the true data distribution either. As a result, the training dynamics are inherently unstable near the equilibrium point.

This phenomenon is general: as long as the data distribution is concentrated on a low dimensional manifold and the class of discriminators is big enough, there is no incentive for the discriminator to produce zero gradients orthogonal to the tangent space of the data manifold and hence converge towards the equilibrium discriminator. Even if the generator produces *exactly* the true data distribution, there is no incentive for the discriminator to produce zero gradients orthogonal to the tangent space. These additional degrees of freedom for the discriminator near the equilibrium point can result in purely imaginary eigenvalues of the Jacobian of the gradient vector field, which prevent convergence of gradient based GAN optimization.

Note that this phenomenon can only arise if the true data distribution is concentrated on a lower dimensional manifold. Indeed, Nagarajan et al. [11] showed that - under some suitable assumptions - gradient descent based GAN optimization is locally convergent for absolutely continuous distributions. Unfortunately, this assumption may not be satisfied for data distributions like natural images to which GANs are commonly applied [1]. Moreover, even if the data distribution is absolutely continuous but concentrated along some lower dimensional manifold, the eigenvalues of the Jacobian of the gradient vector field will then be very close to the imaginary axis, resulting in a highly ill-conditioned problem. This was observed in [10] where the authors examined the spectrum of the Jacobian for a data distribution given by circular mixture of Gaussians with small variance.

3 Regularization strategies

As we have seen in Section 2, unregularized GAN training generally does not converge to the Nash-equilibrium. In this section, we discuss how several regularization techniques that have been proposed in the literature, influence con-

vergence on our example problem.

Interestingly, we find that both instance noise and gradient penalties make the GAN converge, whereas WGAN and WGAN-GP-regularization with a fixed number of discriminator updates and a fixed learning rate do in general not converge to the Nash-equilibrium. The convergence properties of WGANs were also considered in [11] where it is shown that even for absolutely continuous densities and infinitesimal learning rates, the Nash equilibrium in WGANs is generally not exponentially stable.

Interestingly, we also found that the nonsaturating loss proposed in the original GAN paper [3] leads to convergence of the continuous system, albeit with an extremely slow convergence rate.

3.1 Nonsaturating GAN

Especially in the beginning of training, the discriminator can reject samples produced by the generator with high confidence [3]. When this happens, the loss for the generator may saturate so that the generator receives almost no gradient information anymore.

To circumvent this problem Goodfellow et al. [3] introduced a nonsaturating objective for the generator. In nonsaturating GANs, the generator objective is replaced with³

$$\max_{\theta} \mathbb{E}_{p_{\theta}(x)} f(-D_{\psi}(x)). \quad (9)$$

In our example, this is

$$\max_{\theta} f(-\psi\theta). \quad (10)$$

While the nonsaturating generator objective was originally motivated by global stability considerations, we investigate its effect on local convergence. A linear analysis similar to normal GANs yields

Lemma 5. *The unique Nash-equilibrium for the nonsaturating GAN on the example problem is given by $\theta = \psi = 0$. The eigenvalues of the Jacobian of the gradient vector field at the equilibrium are given by $\pm f'(0)i$ which are both on the imaginary axis.*

Lemma 5 implies that simultaneous gradient descent is not locally convergent for a nonsaturating GAN and any learning rate $h > 0$, because the eigenvalues of the Jacobian of the corresponding update operator F_h all have absolute value larger than 1. While Lemma 5 also rules out linear convergence towards the Nash-equilibrium in the continuous case (i.e. for $h \rightarrow 0$), the continuous training dynamics could in principle still converge with a sublinear convergence rate. Indeed, we found this to be the case for our example problem. We have

Lemma 6. *For every integral curve of the gradient vector field of the nonsaturating GAN we have*

$$\frac{d}{dt}(\theta(t)^2 + \psi(t)^2) = 2[f'(\theta\psi) - f'(-\theta\psi)]\theta\psi. \quad (11)$$

³ In [3], the authors consider the standard objective $f(t) = -\log(1 + \exp(-t))$.

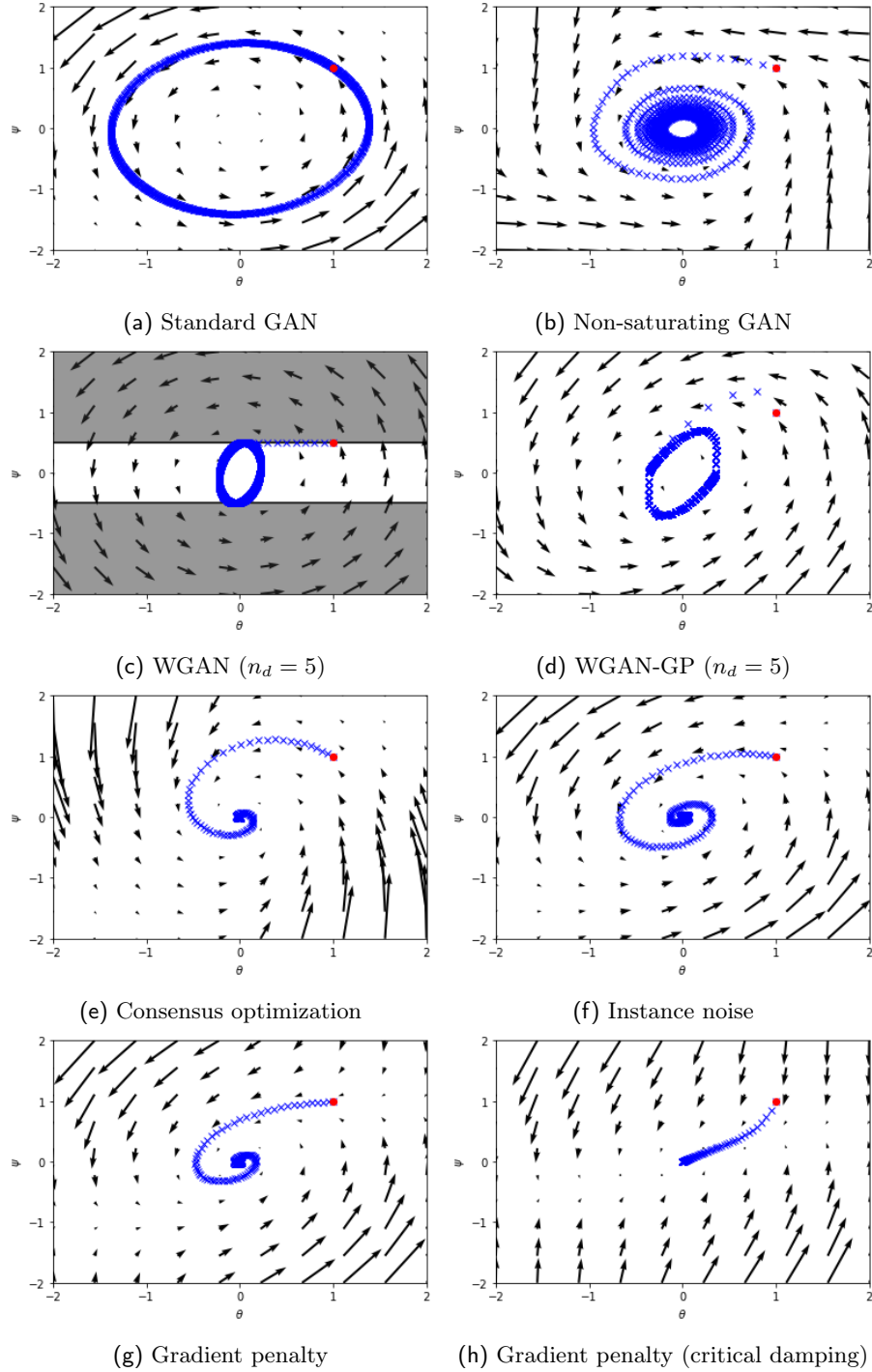


Fig. 3: Convergence properties of different GAN training algorithm using alternating gradient descent with recommended number of discriminator updates per generator update ($n_d = 1$ if not noted otherwise). The grayed out area in Figure 3c visualizes the set of forbidden values for the discriminator parameter ψ .

For concave f this is nonpositive. Moreover, for $f''(0) < 0$, the continuous training dynamics of the nonsaturating GAN in our example problem converge with logarithmic convergence rate.

Note that the standard choice $f(t) = -\log(1 + \exp(-t))$ is concave and satisfies $f''(0) = -\frac{1}{4} < 0$. Lemma 5 is hence applicable and shows that the GAN training dynamics for the standard choice of f converge with logarithmic convergence rate in the continuous case. The training behavior of the nonsaturating GAN on our example problem is visualized in Figure 3b.

3.2 Wasserstein GAN

The two-player GAN game can be interpreted as minimizing a probabilistic divergence between the true data distribution and the distribution produced by the generator [12, 3]. This divergence is obtained by considering the best-response strategy for the discriminator, resulting in an objective function that only contains the generator parameters. Many recent regularization techniques for GANs are based on the observation [1, 2] that this divergence may be discontinuous with respect to the parameters of the generator or may even take on infinite values if the support of the data distribution and the generator distribution do not match. Note, however, that this observation does not imply that there is no equilibrium for the original GAN game nor does it imply that it cannot be computed: it only implies that the equilibrium point cannot be computed by optimizing the discriminator fully to convergence in each iteration followed by one gradient-descent update for the generator.

To make the divergence continuous with respect to the parameters of the generator, Wasserstein GANs (WGANs) [2] replace the Jensen-Shannon divergence used in the original derivation of GANs [3] with the Wasserstein-divergence. As a result, the authors of [2] propose to use $f(t) = t$ and restrict the class of discriminators to Lipschitz continuous functions with Lipschitz constant equal to some $g_0 > 0$. While a WGAN converges if the discriminator is always trained until convergence, in practice WGANs are usually trained by running only a fixed finite number of discriminator updates per generator update. However, near the Nash-equilibrium the optimal discriminator parameters can have a discontinuity as a function of the current generator parameters: in our example problem, the optimal discriminator has to move from $\psi = -1$ to $\psi = 1$ when θ changes signs. As the gradients get smaller near the equilibrium point, the gradient updates do not lead to convergence for the discriminator. Overall, the training dynamics are again determined by the Jacobian of the gradient vector field near the Nash-equilibrium. As a result, we have

Lemma 7. *WGANs trained with simultaneous or alternating gradient descent with a fixed number of generator and discriminator updates and a fixed learning rate $h > 0$ do generally not converge to the Nash equilibrium.*

The training behavior of the WGAN on our example problem is visualized in Figure 3c.

We stress that this analysis only holds if the discriminator is trained with a fixed number of discriminator updates (as it is usually done in practice). More careful training that ensures that the discriminator is kept exactly optimal or two-timescale training [6] might be able to ensure convergence for WGANs. However, these more complex training techniques introduce new hyperparameters (such as an annealing schedule) that might be hard to tune in practice.

3.3 Wasserstein GAN-GP

In practice, it can be hard to enforce the Lipschitz-constraint for WGANs. A practical solution to this problem is given in [4], where a simple gradient penalty with a similar effect as the Lipschitz-constraint is derived. The resulting training objective is commonly referred to as WGAN-GP.

Similarly to WGANs, we found that the training algorithm proposed in WGAN-GP does not converge for our simple example problem. A similar analysis also applies to the DRAGAN-regularizer proposed in [8].

The regularizer considered in [4] is given by

$$R(\psi) = \frac{\gamma}{2} \mathbb{E}_{x_1, x_2 \sim p_D} \mathbb{E}_{\epsilon \sim U[0,1]} (\|\nabla_x D_\psi(\epsilon x_1 + (1 - \epsilon)x_2)\| - g_0)^2.$$

In our example, it simplifies to

$$R(\psi) = \frac{\gamma}{2} (|\psi| - g_0)^2$$

The corresponding gradient vector field is given by

$$\tilde{v}(\theta, \psi) = \begin{pmatrix} -\psi \\ \theta - \text{sign}(\psi)\gamma(|\psi| - g_0) \end{pmatrix}. \quad (12)$$

Note that the gradient vector field has a discontinuity at the equilibrium point, as the gradient vector field takes on values with norm bigger than some fixed constant in every neighborhood of the equilibrium point. As a result, we have

Lemma 8. *WGAN-GP trained with simultaneous or alternating gradient descent with a fixed number of generator and discriminator updates and a fixed learning rate $h > 0$ does generally not converge to the Nash equilibrium.*

The training behavior of WGAN-GP on our example problem is visualized in Figure 3d.

As for WGANs, we stress that this analysis only holds if the discriminator is trained with a fixed number of discriminator updates. Again, more careful training that ensures that the discriminator is kept exactly optimal or two-timescale training [6] might be able to ensure convergence for WGAN-GP.

3.4 Consensus optimization

Consensus optimization [10] is an algorithm that attempts to solve the problem of eigenvalues with zero real-part by introducing a regularization term that

explicitly moves the eigenvalues to the left. The regularization term in consensus optimization is given by

$$R(\theta, \psi) = \frac{\gamma}{2} \|v(\theta, \psi)\|^2 = \frac{\gamma}{2} (\|\nabla_{\theta} L(\theta, \psi)\|^2 + \|\nabla_{\psi} L(\theta, \psi)\|^2). \quad (13)$$

As was proved in [10], consensus optimization converges locally for small step sizes $h > 0$ to the Nash-equilibrium.

Indeed, for our example we have

Lemma 9. *The eigenvalues of the Jacobian of the gradient vector field for consensus optimization at the equilibrium point are given by*

$$\lambda_{1/2} = -\gamma f'(0)^2 \pm i f'(0) \quad (14)$$

In particular, all eigenvalues have a negative real part $-\gamma f'(0)^2$. Hence, simultaneous and alternating gradient descent are both locally convergent using consensus optimization for small enough learning rates.

A visualization of consensus optimization on our example problem is given in Figure 3e.

Unfortunately, consensus optimization has the drawback that it can introduce new spurious points of attraction to the GAN training dynamics. While this is usually not a problem for simple examples, it can be a problem for more complex ones like very deep neural networks.

A similar regularization term as in consensus optimization was also independently proposed in [11]. However, the authors of [11] propose to only regularize the component $\nabla_{\psi} L(\theta, \psi)$ of the gradient vector field corresponding to the discriminator parameters. Moreover, the regularization term is only added to the generator objective to give the generator more foresight. It can be shown [11] that this simplified regularization term also makes the training dynamics locally convergent, but might be better behaved at stationary points of the GAN training dynamics that do not correspond to a local Nash-equilibrium. Indeed, a more detailed analysis shows that this simplified regularization term behaves similarly to instance noise and gradient penalties (which we will discuss in Section 3.5 and Section 3.6) on our example problem.

3.5 Instance noise

A common technique to stabilize GANs is to add *instance noise* [16, 1], i.e. independent Gaussian noise, to the data points. While the original motivation was to make the probabilistic divergence between data and generator distribution well-defined for distributions that do not have common support, this does not clarify the effects of instance noise on the *training algorithm* itself and its ability to find a Nash-equilibrium. Interestingly, however, it was recently shown [11] that in the case of absolutely continuous distributions, gradient descent based GAN optimization is - under suitable assumptions - locally convergent. An explanation for this phenomenon is given in Section 2.3: for absolutely continuous

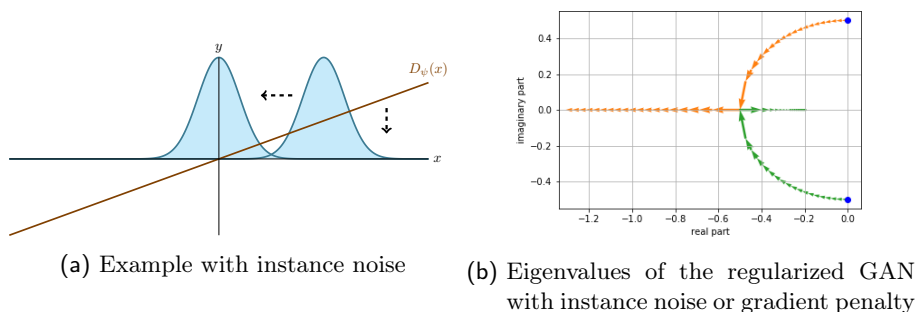


Fig. 4: Simple example of GAN training with instance noise. While unregularized GAN training is inherently unstable, instance noise can stabilize it: near the Nash equilibrium, the discriminator is pushed towards the zero discriminator (left figure), hence creating a radial component in the gradient vector field that corresponds to a negative real part in the eigenvalues (right figure).

densities the equilibrium discriminator is pushed towards the 0-discriminator. This creates a radial component in the gradient vector field which corresponds to eigenvalues with negative real-part (Figure 4).

Indeed, we have for our example problem:

Lemma 10. *When using instance noise with standard deviation σ , the eigenvalues of the Jacobian of the gradient vector field are given by*

$$\lambda_{1/2} = f''(0)\sigma^2 \pm \sqrt{f''(0)^2\sigma^4 - f'(0)^2}. \quad (15)$$

In particular, all eigenvalues of the Jacobian have a negative real-part at the Nash-equilibrium if $f''(0) < 0$. Hence, simultaneous and alternating gradient descent are both convergent for small enough learning rates.

Interestingly, Lemma 10 shows that there is a critical noise level given by $\sigma_{\text{critical}}^2 = |f'(0)|/|f''(0)|$. If the noise level is smaller than the critical noise level, the eigenvalues of the Jacobian have nonzero imaginary part which results in a rotational component in the gradient vector field near the equilibrium point. If the noise level is larger than the critical noise level σ_{critical} , all eigenvalues of the Jacobian become real-valued and the rotational component in the gradient vector field disappears. The optimization problem is best behaved when we select $\sigma = \sigma_{\text{critical}}$: in this case we can even achieve quadratic convergence for $h = |f'(0)|^{-1}$. The effect of instance noise on the eigenvalues is visualized in Figure 4b, which shows the traces of the two eigenvalues as we increase σ from 0 to $2\sigma_{\text{critical}}$.

Figure 3f shows the training behavior of the GAN with instance noise, showing that instance noise indeed creates a strong radial component in the gradient vector field which makes the training algorithm converge.

3.6 Gradient penalty

Motivated by the success of instance noise to make the f -divergence between two distributions well-defined, Roth et al. [14] derived a local approximation to instance noise that results in a gradient penalty for the discriminator.

While the approximation derived in [14] may be loose far away from the true data distribution and for larger regularization parameters, it turns out that it preserves exactly the properties of instance noise with respect to local stability.

In our simple example, a penalty on the squared norm of the gradients of the discriminator (no matter where) results in the regularizer

$$R(\psi) = \frac{\gamma}{2}\psi^2. \quad (16)$$

This regularizer does not include the weighting terms considered in [14]. However, the same analysis can also be applied to the regularizer with the additional weighting, yielding almost exactly the same results.

Lemma 11. *The eigenvalues of the Jacobian of the gradient vector field for the gradient-regularized GAN at the equilibrium point are given by*

$$\lambda_{1/2} = -\frac{\gamma}{2} \pm \sqrt{\frac{\gamma^2}{4} - f'(0)^2}. \quad (17)$$

In particular, all eigenvalues have negative real part. Hence, simultaneous and alternating gradient descent are both locally convergent for small enough learning rates.

Interestingly, gradient penalties have exactly the same effect on local stability as instance noise in our example. In fact, there is an exact equivalence for $\gamma = -2f''(0)\sigma^2$. As for instance noise, there is a critical regularization parameter $\gamma_{\text{critical}} = 2|f'(0)|$ that results in a locally rotation free vector field.

Note, however, that in contrast to instance noise, gradient penalties do not change the distribution to be learned nor do they change the Nash-equilibrium which is highly beneficial for more complex examples.

A visualization of the training behavior of the GAN with gradient penalty is shown in Figure 3g. Figure 3h illustrates the training behavior of the GAN with gradient penalty and critical damping. In particular, we see that near the Nash-equilibrium the vector field does not have a rotational component anymore and hence behaves like a normal optimization problem.

4 A simplified gradient penalty

In the simple example we discussed in this note, the gradient of the discriminator was constant everywhere. Therefore, it does not matter at what data points we evaluate the gradient penalty term discussed in Section 11. While convenient, it does not answer the question of how to implement the regularizer in a more intricate real-world example.

Our analysis suggests that the main effect of the gradient penalty on local stability is to penalize the discriminator from deviating from the Nash-equilibrium. The simplest way to achieve this is to penalize the gradient on real data alone: when the generator distribution produces the true data distribution and the discriminator is equal to 0 on the data manifold, the gradient penalty ensures that the discriminator cannot create a nonzero gradient on the data manifold without suffering a loss in the two-player GAN game.

All in all, this leads to a training objective of the form

$$\min_{\theta} \max_{\psi} \mathbb{E}_{p_{\theta}(x)} [f(D_{\psi}(x))] + \mathbb{E}_{p_{\mathcal{D}}(x)} [f(-D_{\psi}(x))] - \frac{\gamma}{2} \mathbb{E}_{p_{\mathcal{D}}(x)} \|\nabla_x D_{\psi}(x)\|^2. \quad (18)$$

Note that this loss is almost equivalent to the regularizer derived by Roth et al. [14], but does not contain the weighting terms and is only applied to points on the true data distribution.

This gradient penalty can alternatively be interpreted as a way of reducing mode collapse: in the beginning all generated samples are attracted by some regions in the true data distribution. However, as the generator distribution moves closer to these regions, the gradients become smaller, effectively slowing this process down and giving the discriminator time to adapt. Without the gradient penalty in (18), the slope of the discriminator will be high near these regions for a longer period of time. This encourages the generator to aggregate more mass at the mode than needed which can lead to mode collapse. Moreover, penalizing the gradient on the true data distribution makes the generator focus on the samples that are farther away from the true data distribution. This might also help reduce mode collapse and increase sample diversity.

In practice, we found this simple regularizer to be very effective. Some experimental results on the celebA [9] and Imagenet [15] datasets can be found in the appendix.

5 Discussion

In this note, we concentrated on the local stability properties of GAN training. Contrary to current work on the stability properties of GAN training, we found that many of the stability issues can be well explained by looking at its local properties [10, 11]. Nonetheless, we believe that more work needs to be done to understand global convergence.

For example, while consensus optimization leads to local convergence, it can also introduce new spurious points of attraction to the GAN training dynamics. As we have seen, gradient penalties [8, 14] and instance noise [16, 1] can also make GAN training locally convergent, but usually don't have this problem. However, in contrast to gradient penalties, instance noise changes the probability distribution to be learned, making the former the preferable option for most use cases.

Perhaps surprisingly, we found that WGANs [2] and WGAN-GP [4] do not necessarily lead to local convergence if the discriminator is not trained com-

pletely to convergence for every generator update. Especially close to the Nash-equilibrium, this requirement becomes increasingly hard to fulfill, as the optimal discriminator parameters do generally not depend continuously on the current parameters of the generator. It is an open question if these problems also arise in practice and what the implications of these results are.

Based on our local analysis, we also introduced a new simplified gradient penalty term which we found to work well in practice. Despite our encouraging first results, more work needs to be done to understand the benefits and disadvantages of different variants of gradient regularization. In particular, it is not clear yet what kind of gradient regularization works best in practice. While from a local point of view it does not matter whether we penalize the discriminator gradients on the true data distribution, the generator distribution or both, it is possible that there are more fundamental differences regarding global convergence.

6 Conclusion

In this note we analyzed the stability of GAN training on a simple yet prototypical example. Due to the simplicity of the example, we were able to analyze the convergence properties of the training dynamics analytically and we showed that gradient based GAN optimization is in general not convergent. Moreover, we analyzed recent techniques for stabilizing GAN training. Our findings show that WGANs and WGAN-GP do not necessarily lead to local convergence whereas instance noise and gradient penalties do.

While our analysis sheds light on the local convergence properties of GAN training, more work needs to be done to understand global convergence and to answer basic questions about the existence and properties of Nash-equilibria for GANs.

Acknowledgements

I would like to thank Vaishnavh Nagarajan and Kevin Roth for insightful discussions. I also thank Vaishnavh Nagarajan for giving helpful feedback on an early draft of this manuscript. This work was supported by Microsoft Research through its PhD Scholarship Programme.

References

- [1] Martín Arjovsky and Léon Bottou. Towards principled methods for training generative adversarial networks. *CoRR*, abs/1701.04862, 2017.
- [2] Martín Arjovsky, Soumith Chintala, and Léon Bottou. Wasserstein GAN. *CoRR*, abs/1701.07875, 2017.

-
- [3] Ian J. Goodfellow, Jean Pouget-Abadie, Mehdi Mirza, Bing Xu, David Warde-Farley, Sherjil Ozair, Aaron C. Courville, and Yoshua Bengio. Generative adversarial nets. In *Advances in Neural Information Processing Systems 27: Annual Conference on Neural Information Processing Systems 2014, December 8-13 2014, Montreal, Quebec, Canada*, pages 2672–2680, 2014.
 - [4] Ishaan Gulrajani, Faruk Ahmed, Martín Arjovsky, Vincent Dumoulin, and Aaron C. Courville. Improved training of wasserstein gans. In *Advances in Neural Information Processing Systems 30: Annual Conference on Neural Information Processing Systems 2017, 4-9 December 2017, Long Beach, CA, USA*, pages 5769–5779, 2017.
 - [5] Kaiming He, Xiangyu Zhang, Shaoqing Ren, and Jian Sun. Deep residual learning for image recognition. In *Proceedings of the IEEE conference on computer vision and pattern recognition*, pages 770–778, 2016.
 - [6] Martin Heusel, Hubert Ramsauer, Thomas Unterthiner, Bernhard Nessler, and Sepp Hochreiter. Gans trained by a two time-scale update rule converge to a local nash equilibrium. In *Advances in Neural Information Processing Systems 30: Annual Conference on Neural Information Processing Systems 2017, 4-9 December 2017, Long Beach, CA, USA*, pages 6629–6640, 2017.
 - [7] Hassan K Khalil. Nonlinear systems. *Prentice-Hall, New Jersey*, 2(5):5–1, 1996.
 - [8] Naveen Kodali, Jacob D. Abernethy, James Hays, and Zsolt Kira. How to train your DRAGAN. *CoRR*, abs/1705.07215, 2017.
 - [9] Ziwei Liu, Ping Luo, Xiaogang Wang, and Xiaoou Tang. Deep learning face attributes in the wild. In *Proceedings of International Conference on Computer Vision (ICCV)*, 2015.
 - [10] Lars M. Mescheder, Sebastian Nowozin, and Andreas Geiger. The numerics of gans. In *Advances in Neural Information Processing Systems 30: Annual Conference on Neural Information Processing Systems 2017, 4-9 December 2017, Long Beach, CA, USA*, pages 1823–1833, 2017.
 - [11] Vaishnavh Nagarajan and J. Zico Kolter. Gradient descent GAN optimization is locally stable. In *Advances in Neural Information Processing Systems 30: Annual Conference on Neural Information Processing Systems 2017, 4-9 December 2017, Long Beach, CA, USA*, pages 5591–5600, 2017.
 - [12] Sebastian Nowozin, Botond Cseke, and Ryota Tomioka. f-gan: Training generative neural samplers using variational divergence minimization. In *Advances in Neural Information Processing Systems 29: Annual Conference on Neural Information Processing Systems 2016, December 5-10, 2016, Barcelona, Spain*, pages 271–279, 2016.

-
- [13] Alec Radford, Luke Metz, and Soumith Chintala. Unsupervised representation learning with deep convolutional generative adversarial networks. *arXiv preprint arXiv:1511.06434*, 2015.
 - [14] Kevin Roth, Aurélien Lucchi, Sebastian Nowozin, and Thomas Hofmann. Stabilizing training of generative adversarial networks through regularization. In *Advances in Neural Information Processing Systems 30: Annual Conference on Neural Information Processing Systems 2017, 4-9 December 2017, Long Beach, CA, USA*, pages 2015–2025, 2017.
 - [15] Olga Russakovsky, Jia Deng, Hao Su, Jonathan Krause, Sanjeev Satheesh, Sean Ma, Zhiheng Huang, Andrej Karpathy, Aditya Khosla, Michael Bernstein, Alexander C. Berg, and Li Fei-Fei. ImageNet Large Scale Visual Recognition Challenge. *International Journal of Computer Vision (IJCV)*, 115(3):211–252, 2015.
 - [16] Casper Kaae Sønderby, Jose Caballero, Lucas Theis, Wenzhe Shi, and Ferenc Huszár. Amortised MAP inference for image super-resolution. *CoRR*, abs/1610.04490, 2016.

Appendix

Definitions

In this section, we recall some basic definitions from the theory of discrete nonlinear dynamical systems. For a similar description of the theory of continuous nonlinear dynamical systems see for example [7].

In this section we consider continuously differentiable operators $F : \Omega \rightarrow \Omega$ acting on an open set $\Omega \subset \mathbb{R}^n$. A fixed point of F is a point $\bar{x} \in \Omega$ such that $F(\bar{x}) = \bar{x}$. We are interested in stability and convergence of the fixed point iteration $F^{(k)}(x)$ near the fixed point. To this end, we first have to define what we mean by stability and local convergence:

Definition 12. *Let $\bar{x} \in \Omega$ be a fixed point of a continuously differentiable operator $F : \Omega \rightarrow \Omega$. We call \bar{x}*

- *stable if for every $\epsilon > 0$ there is $\delta > 0$ such that $\|x - \bar{x}\| < \delta$ implies $\|F^{(k)}(x) - \bar{x}\| < \epsilon$ for all $k \in \mathbb{N}$.*
- *asymptotically stable if it is stable and there is $\delta > 0$ such that $\|x - \bar{x}\| < \delta$ implies that $F^{(k)}(x)$ converges to \bar{x}*
- *exponentially stable if there is $\lambda \in [0, 1)$, $\delta > 0$ and $C > 0$ such that $\|x - \bar{x}\| < \delta$ implies $\|F^{(k)}(x) - \bar{x}\| < C\|x - \bar{x}\|\lambda^k$ and all $k \in \mathbb{N}$.*

If \bar{x} is asymptotically stable fixed point of F , we call the algorithm obtained by iteratively applying F *locally convergent* towards \bar{x} . If \bar{x} is exponentially stable, we call the corresponding algorithm *linearly convergent*.

Proofs

This section contains the proofs for the results presented in the main paper.

Lemma 1. *The unique equilibrium point of the training objective in (5) is given by $\phi = \psi = 0$. Moreover, the Jacobian of the gradient vector field at the equilibrium point has the two eigenvalues $\pm f'(0)$ which are both on the imaginary axis.*

Proof. The loss in (5) can be rewritten as

$$L(\theta, \psi) = f(\theta \cdot \psi) + \text{const} \quad (19)$$

It is easy to check that the gradient vector field is given by

$$v(\theta, \psi) = \begin{pmatrix} -f'(\theta\psi)\psi \\ f'(\theta\psi)\theta \end{pmatrix}. \quad (20)$$

Because $L(\theta, 0) = L(\psi, 0) = \text{const}$ for all $\theta, \psi \in \mathbb{R}$, $(\theta, \psi) = (0, 0)$ is indeed a Nash-equilibrium for the game defined by (19). Because we assume $f'(t) \neq 0$

for all $t \in \mathbb{R}$, we have $v(\theta, \psi) = 0$ if and only if $(\theta, \psi) = (0, 0)$, showing that $(0, 0)$ is indeed the unique Nash-equilibrium.

Moreover, the Jacobian of v is given by

$$v'(\theta, \psi) = \begin{pmatrix} -f''(\theta\psi)\psi^2 & -f'(\theta\psi) - f''(\theta\psi)\theta\psi \\ f'(\theta\psi) + f''(\theta\psi)\theta\psi & f''(\theta\psi)\theta^2 \end{pmatrix}. \quad (21)$$

Evaluating it at the Nash equilibrium $\theta = \psi = 0$, we obtain

$$v'(0, 0) = \begin{pmatrix} 0 & -f'(0) \\ f'(0) & 0 \end{pmatrix} \quad (22)$$

which has eigenvalues $\pm f'(0)i$. \square

Lemma 2. *The integral curves of the gradient vector field $v(\theta, \psi)$ do not converge to the Nash-equilibrium. More specifically, every integral curve $(\theta(t), \psi(t))$ of the gradient vector field $v(\theta, \psi)$ satisfies*

$$\theta(t)^2 + \psi(t)^2 = \text{const} \quad (7)$$

for all $t \in [0, \infty)$.

Proof. Let $R(\theta, \psi) := \frac{1}{2}(\theta^2 + \psi^2)$. Then

$$\frac{d}{dt}R(\theta(t), \psi(t)) = \theta(t)v_1(\theta(t), \psi(t)) + \psi(t)v_2(\theta(t), \psi(t)) = 0, \quad (23)$$

showing that $R(\theta, \psi)$ is indeed constant for all $t \in [0, \infty)$. \square

Lemma 3. *For simultaneous gradient descent, the Jacobian of the update operator $F_h(\theta, \psi)$ has eigenvalues $\lambda_{1/2} = 1 \pm hf'(0)i$ with absolute values $\sqrt{1 + h^2 f'(0)^2}$ at the Nash equilibrium. Independently of the learning rate, simultaneous gradient descent is therefore not stable near the Nash-equilibrium. Even stronger, for every initial condition and learning rate $h > 0$, the norm of the iterates (θ_k, ψ_k) obtained by simultaneous gradient descent is monotonically increasing.*

Proof. The first part is a direct consequence of the convergence analysis proposed in [10].

To see the the norms of the iterates (θ_k, ψ_k) is monotonically increasing, we just calculate

$$\theta_{k+1}^2 + \psi_{k+1}^2 = (\theta_k - hf'(\theta_k\psi_k)\psi_k)^2 + (\psi_k + hf'(\theta_k\psi_k)\theta_k)^2 \quad (24)$$

$$= \theta_k^2 + \psi_k^2 + h^2 f'(\theta_k\psi_k)^2 (\theta_k^2 + \psi_k^2) \quad (25)$$

$$\geq \theta_k^2 + \psi_k^2. \quad (26)$$

\square

Lemma 4. *For alternating gradient descent with n_g generator and n_d discriminator updates, the Jacobian of the update operator $F_h(\theta, \psi)$ has eigenvalues*

$$\lambda_{1/2} = 1 - \frac{n_g n_d h^2}{2} f'(0)^2 \pm \sqrt{\left(1 - \frac{n_g n_d h^2}{2} f'(0)^2\right)^2 - 1}. \quad (8)$$

For $\sqrt{n_g n_d} h f'(0) \leq 2$, all eigenvalues are hence on the unit circle. Moreover for $\sqrt{n_g n_d} h f'(0) > 2$, there are eigenvalues outside the unit ball.

Proof. The update operators for alternating gradient descent are given by

$$F_1(\theta, \psi) = \begin{pmatrix} \theta - h f'(\theta\psi)\psi \\ \psi \end{pmatrix} \text{ and } F_2(\theta, \psi) = \begin{pmatrix} \theta \\ \psi + h f'(\theta\psi)\theta \end{pmatrix}. \quad (27)$$

Hence, the Jacobians of these operators at 0 are given by

$$F_1'(0, 0) = \begin{pmatrix} 1 & -h f'(0) \\ 0 & 1 \end{pmatrix} \text{ and } F_2'(0, 0) = \begin{pmatrix} 1 & 0 \\ h f'(0) & 1 \end{pmatrix}. \quad (28)$$

As a result, the Jacobian of the combined update operator is given by

$$(F_2^{n_d} \circ F_1^{n_g})'(0, 0) = F_2'(0, 0)^{n_d} \cdot F_1'(0, 0)^{n_g} = \begin{pmatrix} 1 & -n_g h f'(0) \\ n_d h f'(0) & -n_g n_d h^2 f'(0)^2 + 1 \end{pmatrix}. \quad (29)$$

An easy calculation shows that the eigenvalues of this matrix are given by

$$\lambda_{1/2} = 1 - \frac{n_g n_d h^2}{2} f'(0)^2 \pm \sqrt{\left(1 - \frac{n_g n_d h^2}{2} f'(0)^2\right)^2 - 1} \quad (30)$$

which are on the unit circle if

$$\sqrt{n_g n_d} h f'(0) < 2. \quad (31)$$

□

Lemma 5. *The unique Nash-equilibrium for the nonsaturating GAN on the example problem is given by $\theta = \psi = 0$. The eigenvalues of the Jacobian of the gradient vector field at the equilibrium are given by $\pm f'(0)i$ which are both on the imaginary axis.*

Proof. The gradient vector field for the nonsaturating GAN is given by

$$v(\theta, \psi) = \begin{pmatrix} -f'(-\theta\psi)\psi \\ f'(\theta\psi)\theta \end{pmatrix}. \quad (32)$$

As in the proof of Lemma 1, we see that $(\psi, \theta) = (0, 0)$ defines the unique Nash-equilibrium for the nonsaturating GAN.

Moreover, the Jacobian is given by

$$v'(\theta, \psi) = \begin{pmatrix} f''(-\theta\psi)\psi^2 & -f'(-\theta\psi) + f''(-\theta\psi)\theta\psi \\ f'(\theta\psi) + f''(\theta\psi)\theta\psi & f''(\theta\psi)\theta^2 \end{pmatrix}. \quad (33)$$

At $\theta = \psi = 0$ we therefore have

$$v'(0,0) = \begin{pmatrix} 0 & -f'(0) \\ f'(0) & 0 \end{pmatrix}. \quad (34)$$

with eigenvalues $\lambda_{1/2} = \pm f'(0)i$. \square

Lemma 6. *For every integral curve of the gradient vector field of the nonsaturating GAN we have*

$$\frac{d}{dt}(\theta(t)^2 + \psi(t)^2) = 2[f'(\theta\psi) - f'(-\theta\psi)]\theta\psi. \quad (11)$$

For concave f this is nonpositive. Moreover, for $f''(0) < 0$, the continuous training dynamics of the nonsaturating GAN in our example problem converge with logarithmic convergence rate.

Proof. The gradient vector field for the nonsaturating GAN is given by

$$v(\theta, \psi) = \begin{pmatrix} -f'(-\theta\psi)\psi \\ f'(\theta\psi)\theta \end{pmatrix}. \quad (35)$$

Hence, we have

$$\frac{d}{dt}(\theta(t)^2 + \psi(t)^2) = v_1(\theta, \psi)\theta + v_2(\theta, \psi)\psi = 2\theta\psi[f'(\theta\psi) - f'(-\theta\psi)]. \quad (36)$$

For concave f , we have

$$\frac{f'(\theta\psi) - f'(-\theta\psi)}{2\theta\psi} \leq 0 \quad (37)$$

and hence

$$\frac{d}{dt}(\theta(t)^2 + \psi(t)^2) \leq 0. \quad (38)$$

Now assume that $f'(0) \neq 0$ and $f''(0) < 0$.

To intuitively understand why the continuous system converges with logarithmic convergence rate, note that near the equilibrium point we asymptotically have in polar coordinates $(\theta, \psi) = (\sqrt{w} \cos(\phi), \sqrt{w} \sin(\phi))$ near the equilibrium point:

$$\dot{\phi} = f'(0) + \mathcal{O}(|w|^{1/2}) \quad (39)$$

$$\dot{w} = 4f''(0)\theta^2\psi^2 + \mathcal{O}(|\theta\psi|^3) = f''(0)w^2 \sin^2(2\phi) + \mathcal{O}(|w|^3). \quad (40)$$

When we ignore higher order terms, we can solve this system explicitly⁴ for ϕ and w :

$$\phi(t) = f'(0)(t - t_0) \quad (42)$$

$$w(t) = \frac{2}{-f''(0)(t - t_0) + \frac{f''(0)}{4f'(0)} \sin(4f'(0)(t - t_0)) + c} \quad (43)$$

⁴ For solving the ODE we use the *separation of variables*-technique and the identity

$$\int 2 \sin^2(ax) dx = x - \frac{\sin(2ax)}{2a}. \quad (41)$$

The training dynamics are hence convergent with logarithmic convergence rate $\mathcal{O}\left(\frac{1}{\sqrt{t}}\right)$.

For a more formal proof, first note that w is nonincreasing by the first part of the proof. Moreover, for every $\epsilon > 0$ there is $\delta > 0$ such that for $w < \delta$:

$$f'(0) - \epsilon \leq \dot{\phi} \leq f'(0) + \epsilon \quad \text{and} \quad \dot{w} \leq (f''(0) \sin^2(2\phi) + \epsilon)w^2. \quad (44)$$

This implies that for every time interval $[0, T]$, $\phi(t)$ is in

$$\bigcup_{k \in \mathbb{Z}} \left[\frac{\pi}{8} + k\frac{\pi}{2}, \frac{3\pi}{8} + k\frac{\pi}{2} \right] \quad (45)$$

for t in a union of intervals $Q_T \subseteq [0, T]$ with total length at least $\beta[\alpha T]$ with some constants $\alpha, \beta > 0$ which are independent of T .

For these $t \in Q_T$ we have $\sin^2(2\phi(t)) \geq \frac{1}{2}$. This shows

$$\dot{w}(t) \leq \left(\frac{1}{2}f''(0) + \epsilon \right) w(t)^2 \quad (46)$$

for $t \in Q_T$ and ϵ small enough. Solving the right hand formally yields

$$w(t) \leq \frac{1}{-\left(\frac{1}{2}f''(0) + \epsilon\right)t + c}. \quad (47)$$

As $w(t)$ is nonincreasing for $t \notin Q_T$ and the total length of Q_T is at least $\beta[\alpha T]$ this shows that

$$w(T) \leq \frac{1}{-\left(\frac{1}{2}f''(0) + \epsilon\right)\beta[\alpha T] + c}. \quad (48)$$

The training dynamics hence converge with logarithmic convergence rate $\mathcal{O}\left(\frac{1}{\sqrt{t}}\right)$. \square

Lemma 7. *WGANs trained with simultaneous or alternating gradient descent with a fixed number of generator and discriminator updates and a fixed learning rate $h > 0$ do generally not converge to the Nash equilibrium.*

Proof. First, consider simultaneous gradient descent. Assume that the iterates (θ_k, ψ_k) converge towards the equilibrium point $(0, 0)$. Note that $(\theta_{k+1}, \psi_{k+1}) \neq 0$ if $(\theta_k, \psi_k) \neq 0$. We can therefore assume without loss of generality that $(\theta_k, \psi_k) \neq 0$ for all $k \in \mathbb{N}$.

Because $\lim_{k \rightarrow \infty} \psi_k = 0$, there exists k_0 such that for all $k \geq k_0$ we have $|\psi_k| < 1$. For $k \geq k_0$ we therefore have

$$\begin{pmatrix} \theta_{k+1} \\ \psi_{k+1} \end{pmatrix} = \begin{pmatrix} 1 & -h \\ h & 1 \end{pmatrix} \begin{pmatrix} \theta_k \\ \psi_k \end{pmatrix}. \quad (49)$$

For $k \geq k_0$, the iterates are therefore given by

$$\begin{pmatrix} \theta_k \\ \psi_k \end{pmatrix} = A^{k-k_0} \begin{pmatrix} \theta_{k_0} \\ \psi_{k_0} \end{pmatrix} \quad \text{with} \quad A = \begin{pmatrix} 1 & -h \\ h & 1 \end{pmatrix}. \quad (50)$$

However, the eigenvalues of A are given by $\lambda_{1/2} = 1 \pm hi$ which both have absolute value $\sqrt{1+h^2} > 1$. This contradicts the assumption that (θ_k, ψ_k) converges to $(0, 0)$.

A similar argument also hold for alternating gradient descent. In this case, A is given by

$$A = \begin{pmatrix} 1 & 0 \\ h & 1 \end{pmatrix}^{n_d} \cdot \begin{pmatrix} 1 & -h \\ 0 & 1 \end{pmatrix}^{n_g} = \begin{pmatrix} 1 & -hn_g \\ hn_d & 1 - h^2n_gn_d \end{pmatrix}. \quad (51)$$

In this case, the eigenvalues of A as in (51) are given by

$$1 - \frac{h^2n_gn_h}{2} \pm \sqrt{\left(1 - \frac{h^2n_gn_h}{2}\right)^2 - 1}. \quad (52)$$

At least one of these eigenvalues has absolute value greater or equal to 1. Note that for almost all initial conditions (θ_0, ψ_0) , the the inner product between the eigenvector corresponding to the eigenvalue with modulus bigger than 1 will be nonzero for all $k \in \mathbb{N}$. Since the recursion in (49) is linear, this contradicts the fact that $(\theta_k, \psi_k) \rightarrow (0, 0)$, showing that alternating gradient descent generally does not converge to the Nash-equilibrium either. \square

Lemma 8. *WGAN-GP trained with simultaneous or alternating gradient descent with a fixed number of generator and discriminator updates and a fixed learning rate $h > 0$ does generally not converge to the Nash equilibrium.*

Proof. First, consider simultaneous gradient descent. Assume that the iterates (θ_k, ψ_k) converge towards the equilibrium point $(0, 0)$. For almost all initial conditions⁵ we have $(\theta_k, \psi_k) \neq (0, 0)$ for all $k \in \mathbb{N}$. This implies

$$|\psi_{k+1} - \psi_k| = h|\theta_k - \gamma\psi_k - \text{sign}(\psi_k)g_0| \rightarrow h|g_0| \neq 0 \quad (53)$$

for $k \rightarrow \infty$, showing that (θ_k, ψ_k) is not a Cauchy sequence. This contradicts the assumption that (θ_k, ψ_k) converges to the equilibrium point $(0, 0)$.

A similar argument also holds for alternating gradient descent. \square

Lemma 9. *The eigenvalues of the Jacobian of the gradient vector field for consensus optimization at the equilibrium point are given by*

$$\lambda_{1/2} = -\gamma f'(0)^2 \pm i f'(0) \quad (14)$$

In particular, all eigenvalues have a negative real part $-\gamma f'(0)^2$. Hence, simultaneous and alternating gradient descent are both locally convergent using consensus optimization for small enough learning rates.

Proof. As shown in [10], the Jacobian of the modified vector field \tilde{v} at the equilibrium point is given by

$$\tilde{v}'(0, 0) = v'(0, 0) - \gamma v'(0, 0)^\top v'(0, 0). \quad (54)$$

⁵ Depending on γ , h and g_0 modulo a set of measure 0.

In our case, this is

$$\tilde{v}'(0,0) = \begin{pmatrix} -\gamma f'(0)^2 & -f'(0) \\ f'(0) & -\gamma f'(0)^2 \end{pmatrix} \quad (55)$$

A simple calculation shows that the eigenvalues of $\tilde{v}'(0,0)$ are given by

$$\lambda_{1/2} = -\gamma f'(0)^2 \pm i f'(0). \quad (56)$$

□

Lemma 10. *When using instance noise with standard deviation σ , the eigenvalues of the Jacobian of the gradient vector field are given by*

$$\lambda_{1/2} = f''(0)\sigma^2 \pm \sqrt{f''(0)^2\sigma^4 - f'(0)^2}. \quad (15)$$

In particular, all eigenvalues of the Jacobian have a negative real-part at the Nash-equilibrium if $f''(0) < 0$. Hence, simultaneous and alternating gradient descent are both convergent for small enough learning rates.

Proof. When using instance noise, the GAN training objective (1) is given by

$$\mathbb{E}_{\tilde{\theta} \sim \mathcal{N}(\theta, \sigma^2)} [f(\tilde{\theta}\psi)] + \mathbb{E}_{x \sim \mathcal{N}(0, \sigma^2)} [f(-x\psi)]. \quad (57)$$

The corresponding gradient vector field is hence given by

$$\tilde{v}(\theta, \psi) = \mathbb{E}_{\tilde{\theta}, x} \begin{pmatrix} -\psi f'(\tilde{\theta}\psi) \\ \tilde{\theta} f'(\tilde{\theta}\psi) - x f'(-x\psi) \end{pmatrix}. \quad (58)$$

The Jacobian is given by

$$\tilde{v}'(\theta, \psi) = \mathbb{E}_{\tilde{\theta}, x} \begin{pmatrix} -f''(\tilde{\theta}\psi)\psi^2 & -f'(\tilde{\theta}\psi) - f''(\tilde{\theta}\psi)\tilde{\theta}\psi \\ f'(\tilde{\theta}\psi) + f''(\tilde{\theta}\psi)\tilde{\theta}\psi & f''(\tilde{\theta}\psi)\tilde{\theta}^2 + x^2 f'(-x\psi) \end{pmatrix} \quad (59)$$

Evaluating it at $\theta = \psi = 0$ yields

$$\tilde{v}'(0,0) = \begin{pmatrix} 0 & -f'(0) \\ f'(0) & 2f''(0)\sigma^2 \end{pmatrix} \quad (60)$$

whose eigenvalues are given by

$$\lambda_{1/2} = f''(0)\sigma^2 \pm \sqrt{f''(0)^2\sigma^4 - f'(0)^2}. \quad (61)$$

□

Lemma 11. *The eigenvalues of the Jacobian of the gradient vector field for the gradient-regularized GAN at the equilibrium point are given by*

$$\lambda_{1/2} = -\frac{\gamma}{2} \pm \sqrt{\frac{\gamma^2}{4} - f'(0)^2}. \quad (17)$$

In particular, all eigenvalues have negative real part. Hence, simultaneous and alternating gradient descent are both locally convergent for small enough learning rates.

Proof. The regularized gradient vector field becomes

$$\tilde{v}(\theta, \psi) = \begin{pmatrix} -f'(\theta\psi)\psi \\ f'(\theta\psi)\theta - \lambda\psi \end{pmatrix}. \quad (62)$$

The Jacobian is therefore given by

$$\tilde{v}'(\theta, \psi) = \begin{pmatrix} -f''(\theta\psi)\psi^2 & -f'(\theta\psi) - f''(\theta\psi)\theta\psi \\ f'(\theta\psi) + f''(\theta\psi)\theta\psi & f''(\theta\psi)\theta^2 - \lambda \end{pmatrix}. \quad (63)$$

Evaluating it at $\theta = \psi = 0$ yields

$$\tilde{v}'(0, 0) = \begin{pmatrix} 0 & -f'(0) \\ f'(0) & -\lambda \end{pmatrix} \quad (64)$$

whose eigenvalues are given by

$$\lambda_{1/2} = -\frac{\lambda}{2} \pm \sqrt{\frac{\lambda^2}{4} - f'(0)^2}. \quad (65)$$

□

Additional experimental results

Figure 5 and Figure 6 show the results obtained by training a GAN with the simplified gradient penalty from Section 4 on the celebA [9] and the Imagenet [15] datasets. For both experiments, we used a regularization parameter of $\gamma = 10$, a batchsize of 64 and RMSProp with learning rate 10^{-4} . We trained the GAN for 150k iterations for celebA and 400k iterations for Imagenet. Moreover, for Imagenet we additionally reduced the learning rate to $2 \cdot 10^{-5}$ after about 300k iterations.

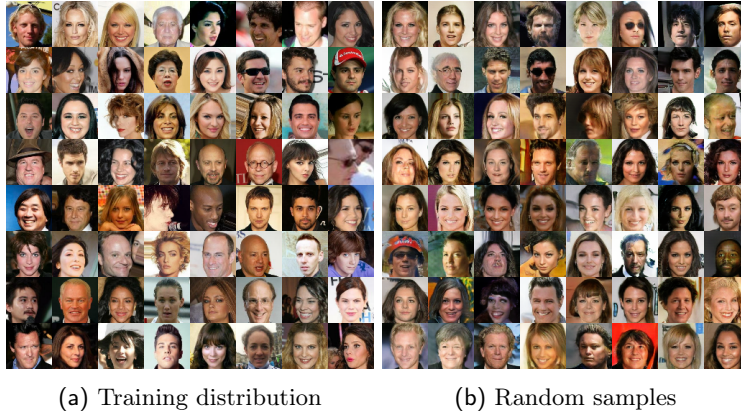


Fig. 5: Results on the celebA dataset [9] (64×64) for a DC-GAN [13] based architecture with additional residual connections [5]. For both the generator and the discriminator, we did not use batch normalization and used a constant number of filters in each layer.



Fig. 6: Results on the Imagenet dataset [15] (64×64) for a DC-GAN [13] based architecture with additional residual connections [5]. For each scale, we add three residual blocks for both the generator and the discriminator. We did not use batch normalization for either the generator nor the discriminator. We use labels by concatenating the input features to both the generator and discriminator with a 256 dimensional embedding of the labels.

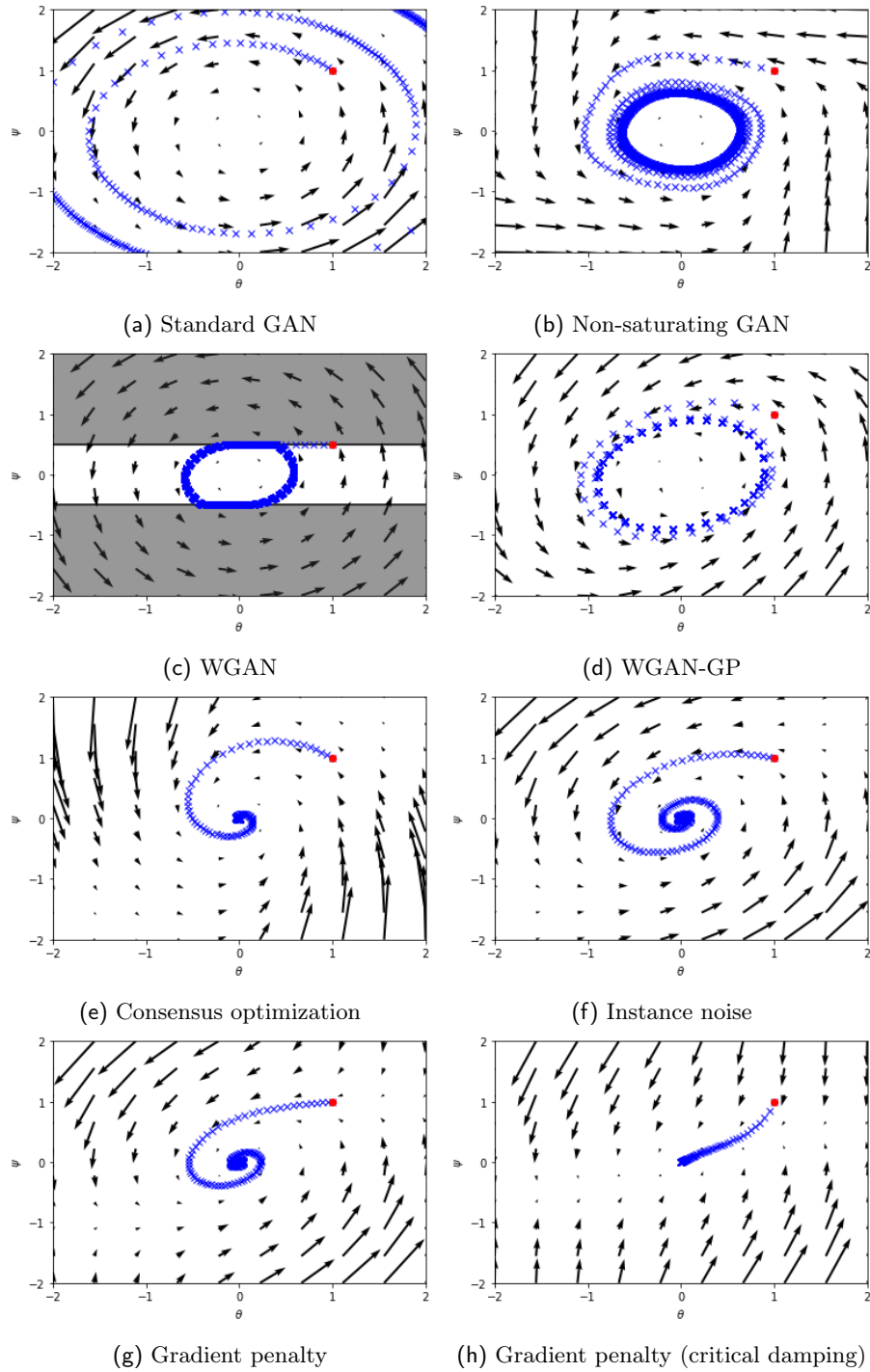


Fig. 7: Convergence properties of different GAN training algorithm using simultaneous gradient descent. The grayed out area in Figure 7c visualizes the set of forbidden values for the discriminator parameter ψ .

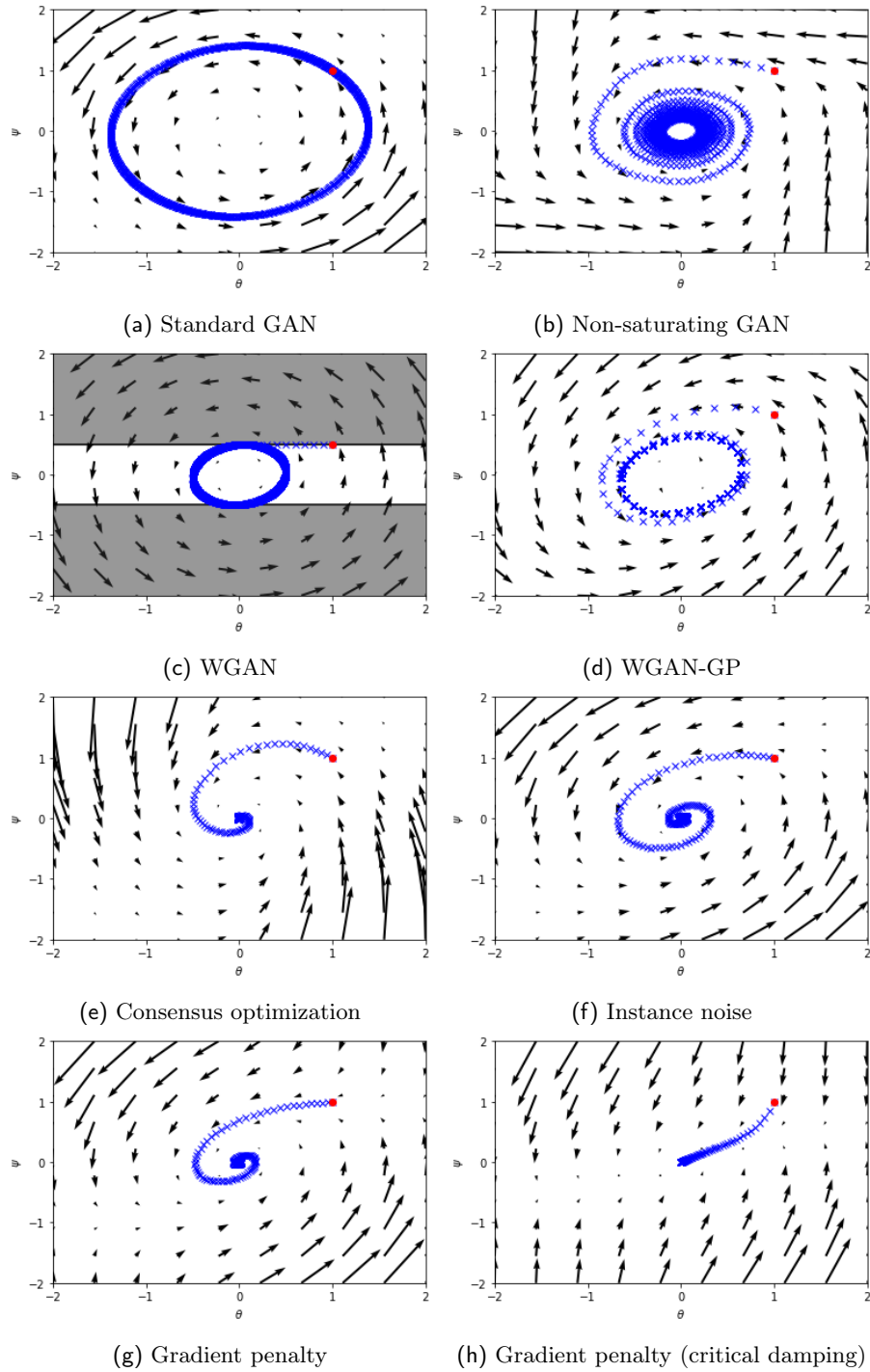


Fig. 8: Convergence properties of different GAN training algorithm using alternating gradient descent with 1 discriminator update per generator update. The grayed out area in Figure 8c visualizes the set of forbidden values for the discriminator parameter ψ .

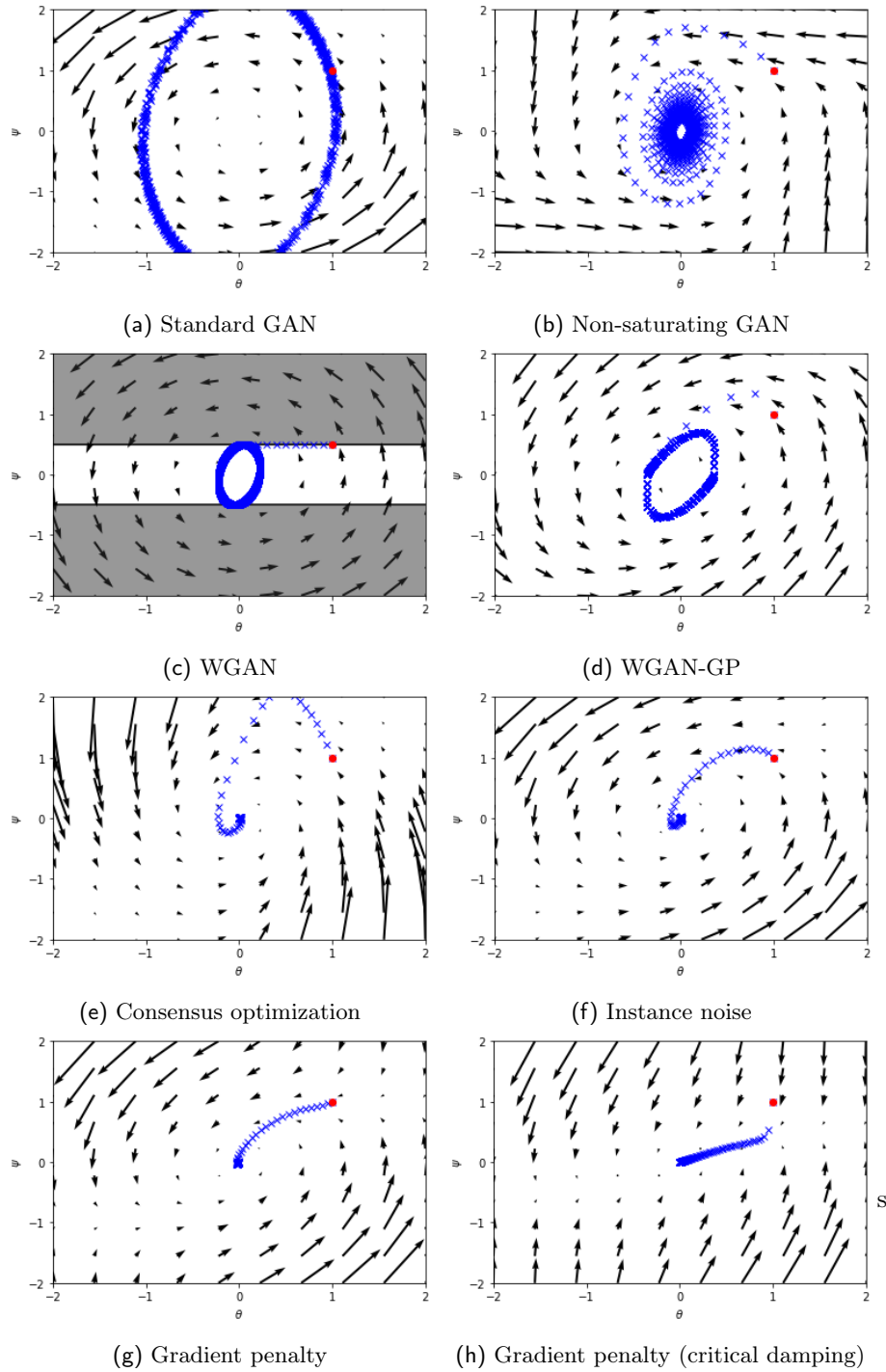


Fig. 9: Convergence properties of different GAN training algorithm using alternating gradient descent with 5 discriminator updates per generator update. The grayed out area in Figure 9c visualizes the set of forbidden values for the discriminator parameter ψ .

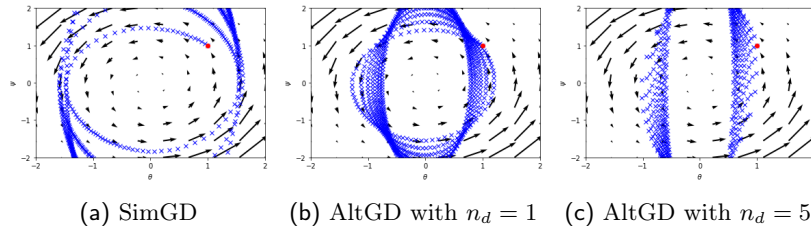


Fig. 10: Convergence properties of our GAN using two time-scale training as proposed in [6]. On our example problem, we did not see any sign of convergence when training with two time-scales.